Int. J. Electrochem. Sci., 8 **(2013)** 4986 - 4995

International Journal of
ELECTROCHEMICAL
SCIENCE
www.electrochemsci.org

Effect of Na_3AlF_6 on the Structure and Mechanical Properties of Plasma Electrolytic Oxidation Coatings on 6061 Al alloy

Xiaodong Wang, Xiaohong Wu, Rui Wang[*], *Zhaozhong Qiu*

School of Chemical Engineering and Technology, Harbin Institute of Technology, Heilongjiang 150001, PR China
[*]E-mail: wangrui001@hit.edu.cn

Received: 16 January 2013 / *Accepted:* 22 February 2013 / *Published:* 1 April 2013

The composition of electrolyte plays a key role in determining the structure and properties of the ceramic coatings by the prepared plasma electrolytic oxidation (PEO) process. In this paper, the effect of Na_3AlF_6 on the properties of PEO coating formed on 6061 Al alloy was explored. The thickness, micro-morphology, structure and mechanical properties of the coatings were studied by eddy current coating thickness gauge, scanning electron microscope (SEM), X-ray diffraction (XRD), and nanoindentation measurements. Our results indicate that the coatings were mainly composed of α-Al_2O_3 and γ-Al_2O_3, there were many micro-pore and pancakes distributing on the surface. After the Na_3AlF_6 was added, the coatings got more compact and the content of α-Al_2O_3 and γ-Al_2O_3 was increased. Meanwhile, the micro-hardness of coatings was increased. With Na_3AlF_6, The coatings showed excellent mechanical properties. The micro-hardness and Young's modulus is 21.363 GPa and 358.067 GPa, respectively. The elastic recovery was 48.76%.

Keywords: Plasma electrolytic oxidation; 6061 Al alloys; Na_3AlF_6; Mechanical properties.

1. INTRODUCTION

In recent years, considerable research efforts have been devoted to design advanced materials with lightweight but also with superior mechanical strength due to the urgent need for a variety of applications including in automotive and aerospace industries [1–5]. 6061 Al alloys, in particular, have been studied extensively because of their unique properties such as high strength/weight ratio, good corrosion resistance, excellent weldability and deformability [6-8]. However, their limited surface hardness and wear resistance have significantly restricted their practical applications. Up to now, various surface engineering techniques, including physical vapor deposition (PVD) [9, 10], thermal spraying [11] and hard anodizing [12-15], have been designed to overcome these problems. However,

the coatings prepared by the PVD process are usually suffer from limited tribological performances and are too thin to support heavy loads and protect the substrate at the contact points due to the elastic and plastic deformation of the substrate under mechanical loading. Coatings prepared by the hard anodizing and thermal spraying approaches have low load of the underlying material and insufficient adhesion, which reduces their durability [16]. More importantly, most of the methods mentioned above involve high temperature during processing, which inevitably degrade the coating and substrate and hence, they are not well suitable for the deposition of alumina coatings on low-melting-point substrates, such as Al alloys.

Plasma electrolytic oxidation (PEO), also called micro arc oxidation (MAO), anodic spark deposition (ASD) or micro plasma oxidation (MPO), is a promising surface treatment technology developed recently. PEO is a complex process that combines electrochemical oxidation with oxide film formation, dissolution and dielectric breakdown. With PEO, the composition and structure of coating can be engineered readily by controlling the electrolyte composition and concentration. PEO works at much lower voltage compared with the conventional anodic oxidation process due to the introduction of the work zone into the high-voltage discharge zone and the ceramic coatings are formed directly on the surface of substrates with the assistance of the high instant temperature and pressure in the micro zone. Hence, the coatings are grow in situ and formed directly on the surface of substrate, which can remarkably enhance the surface properties, including wear resistance, corrosion resistance, and especially adhesion for post coats [17-19].

So far, most of previous researches have focused on applying PEO technique on processing the Al-Cu [20], Al-Si alloys [21], but the Al-Mg alloys are seldom studied. In this paper, we studied the PEO coatings formed on the 6061 Al alloy by using Na_3AlF_6 as the additive. The composition, microstructure, micro-hardness and Young's modulus of the produced ceramic coating were also examined.

2. EXPERIMENTAL

Polished square samples (20 mm × 20 mm × 1 mm) made of 6061 Al alloy (mass fraction: 0.4~0.8% Si, 0.7% Fe, 0.15~0.4% Cu, 0.15% Mn, 0.8~1.2% Mg, 0.04~0.35% Cr, 0.25% Zn, 0.15% Ti, balance Al) were used as the substrate in this study. Prior to PEO treatment, the substrates were ultrasonically degreased in acetone and distilled water. A conducting wire was mounted on one surface of the square sample for external circuit connection. Then, this surface was sealed with insulating lacquer for protection purpose. During the PEO process, the substrates were totally immersed in the electrolyte. A water-cooled electrobath made of stainless steel was used both as the electrolyte container and the counter electrode. A homemade pulsed bipolar electrical source with power of 5 kW was used as the power source. The reaction temperature was controlled below 35°C with cooling water flow. The electronic power frequency was fixed at 50 Hz. The duty ratios of both pulses were equal to 45%. The ratio between the anodic and the cathodic current was set as 1. The entire process was carried out in 50 min under the current density of 10 A/dm^2. An aqueous solution consisting of sodium silicate (10 g/L) and potassium hydroxide (1 g/L) was used as the basic electrolyte. Na_3AlF_6 with

concentration of 0.5 g/L was added into the basic electrolyte as the additive. Control experiments without Na_3AlF_6 additive was also carried out. After the PEO treatment, the samples with surface coatings were rinsed with distilled water and dried in the air.

The thickness of the coatings was measured by an eddy current based thickness gauge (CTG-10, Time Company, China) with the resolution of 1 μm and accuracy of 0.1 μm. In this experiment, the average thickness of each sample was obtained from 10 measurements at different position. The phase composition of the coatings was examined with a RICOH D/max-rB automatic XRD using a Cu Kα source. The surface and cross-section morphology of the coatings was studied by scanning electron microscopy (SEM; Hitachi S-570). The mechanical properties of the coatings were measured by a nanoindenter XP system (Nano Instruments, MTS Systems Corporation, USA) with a Berkovich diamond indenter. All the measurements were made with 500nm penetration depth. Typically 5 indents were obtained for each specimen, from which average values were calculated.

3. RESULTS AND DISCUSSION

3.1. Voltage-time response

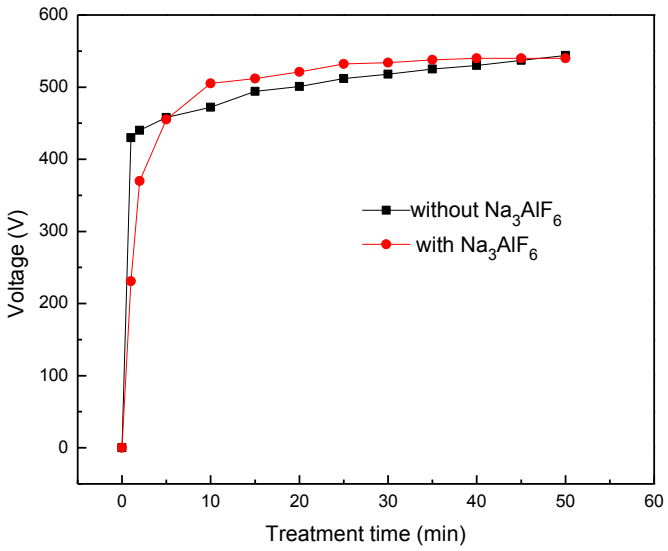

Figure 1. Voltage-time response for PEO coatings.

Fig. 1 shows the variation of the anodic voltage as the function of treatment time during the PEO process in the electrolyte with and without Na_3AlF_6. It can be seen that they have the similar trend on the change of voltage-time curves, with a shape increase of voltage initially but quickly stabilize with the passage of time. However, difference exists regarding to how fast the voltage change. Without Na_3AlF_6 added, the voltage increased approximately linearly at voltage up to 430V at 7 V/s. In contrast, these two parameters were only 370V and 3 V/s with the Na_3AlF_6 additive. During the first 5 min of the PEO process, the anodic voltage in the solution with Na_3AlF_6 was lower[22-24], the

anodic voltages all reach a value of 450 V at 5 min. Afterwards, the anodic voltage in the solution with Na_3AlF_6 was always higher.

3.2 Thickness-time response

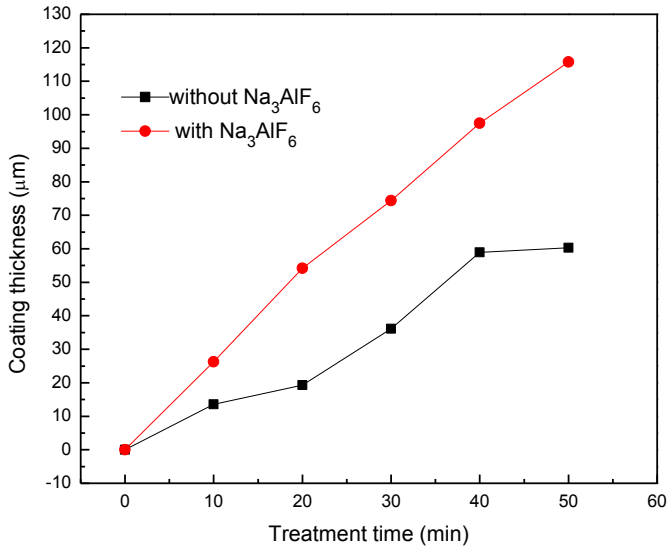

Figure 2. PEO coatings thickness as a function of treatment time.

Fig.2 represents the variation of thickness of PEO coatings with treatment time. It can be seen that the coating thickness increases with the increased treatment time. The effect of Na_3AlF_6 on the coating thickness was obvious[25,26]. The thickness of the coatings obtained in electrolyte without Na_3AlF_6 is about 60 μm, while with Na_3AlF_6 is about 115 μm. This implied that AlF_6^{3-} ion might take part in the PEO process. Considering the anodic voltages in electrolytes with Na_3AlF_6 were higher than the ones without Na_3AlF_6 during the initial PEO process, we believe Na_3AlF_6 is also able to accelerate the formation of coating.

3.3 Morphologies and phase composition of the coatings

Fig. 3 (a) and (d) shows the SEIM images of the PEO coatings formed in electrolyte without and with Na_3AlF_6. As can be seen from this figure, both of these coatings have a large amount of micropores and some microcracks. The micropores are the residual discharge channels during the plasma spark reaction, while the microcracks were caused by the thermal stress due to the rapid solidification of molten oxide in the cool electrolyte. It is obvious that some sintered material like "pancakes" were formed around the micropores. Such material was the molten oxide sputtered out from sparking channels and rapidly solidified by the surrounded electrolyte[27-29]. Comparing (a) and (d), it can be found that with the addition of Na_3AlF_6, the size and the density of the pores decreased

obviously, Fig. 3 (b, c) and (e, f) are the SEM images of the PEO coatings of the surfaces that are polished to about 40 μm and 30 μm from the surface, respectively.

For the coatings prepared in electrolyte without Na_3AlF_6, there are some micropores distributed on the coating for both 40 μm and 30 μm. However, for the coating obtained in electrolyte with Na_3AlF_6 polished to about 30 μm, almost no ovious micropores was found.

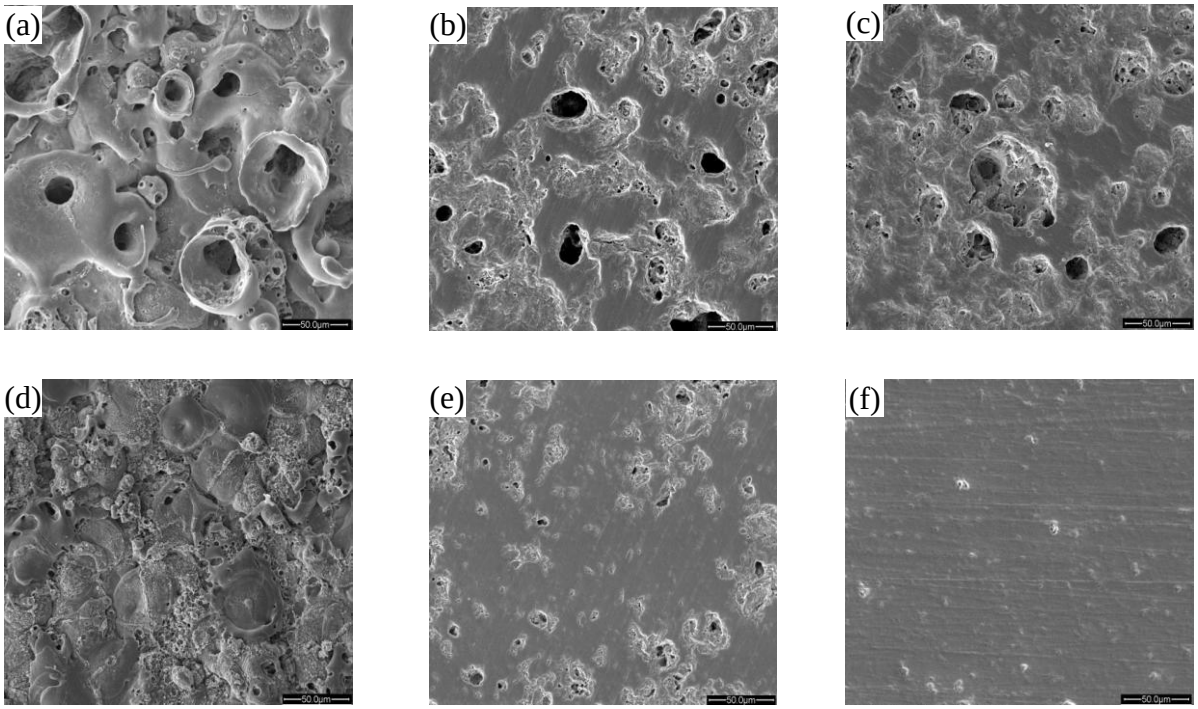

Figure 3. Surface morphologies of the PEO coatings: without Na_3AlF_6 (a) surface, (b) 40μm, (c) 30μm; with Na_3AlF_6 (d) surface (e) 40μm, (f) 30μm.

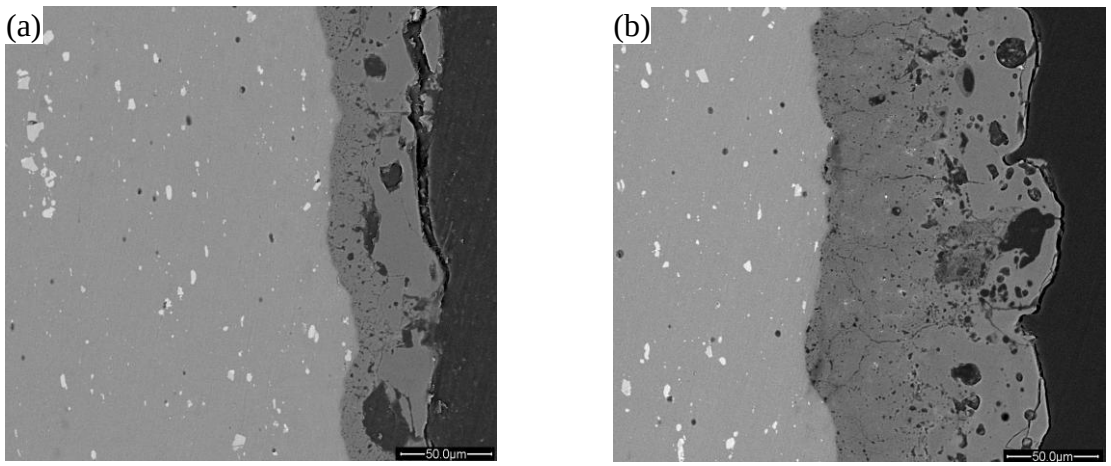

Figure 4. Cross-section morphologies of the PEO coatings: (a) without Na_3AlF_6, (b) with Na_3AlF_6

These results indicated that Na_3AlF_6 was beneficial to decrease the pore quantity and make the coatings more compact. For many industrial applications, dense and homogeneous layers with good mechanical properties are desired. So the research aims at reducing and limiting the growth of the porous layer during PEO. Cross-section morphologies of the PEO coatings are illustrated in Fig. 4. It shows that the coatings were composed by porous outer layers and compact inner layers. There is no obvious discontinuity between the coating and the substrate, implying a good adhesion with substrates. There are some micropores and microcracks in the coatings, but they are neither connected with each other nor penetrated through the whole coatings. The thickness of the coatings obtained in electrolyte without Na_3AlF_6 was about 55μm, however, that obtained in electrolyte with Na_3AlF_6 was about 110μm. It can be concluded that adding Na_3AlF_6 could greatly increase the thickness of the coating.

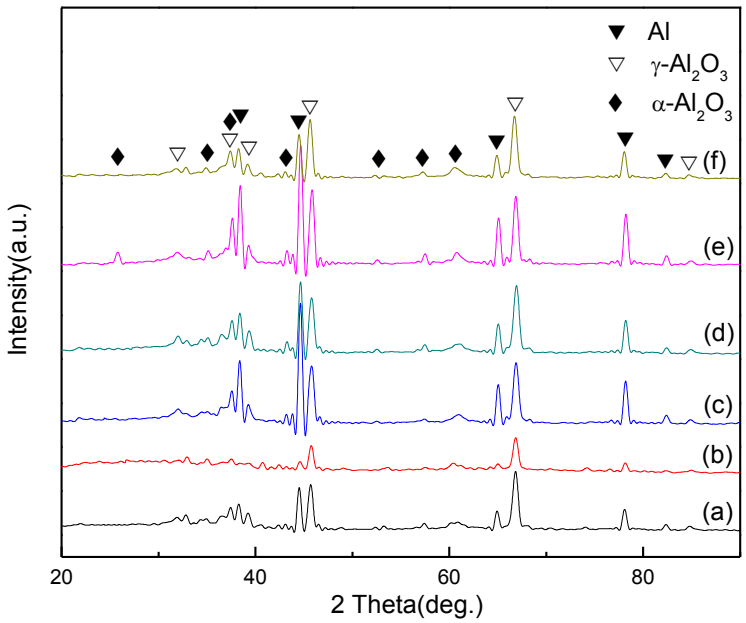

Figure 5. XRD patterns of the PEO coatings: without Na_3AlF_6 (a) surface, (c) 30μm, (d) 40μm; with Na_3AlF_6 (b) surface, (e) 30μm, (f) 40μm.

Fig.5 displays the XRD patterns of the PEO coatings. It can be seen that the coatings were all consisted of α-Al_2O_3 and γ-Al_2O_3, and the diffraction peaks from γ-Al_2O_3 are stronger than those from the α-Al_2O_3. Such differences could be attribute to that α-Al_2O_3 is thermodynamically more stable at all temperatures and γ-Al_2O_3 is metastable and could transform to the α-Al_2O_3 phase at temperature higher than 1273 K. The α-Al_2O_3 phase not easily forming, therefore, the diffraction intensity of α-Al_2O_3 peak is very low. Furthermore, we also detected the peaks from Al in all coatings, because the X-rays can penetrate the coatings and arrive the substrate. With the addition of Na_3AlF_6, it can be seen that the peak intensity of Al decreases, as revealed in Fig. 4 (a, b), while the peak intensity of γ-Al_2O_3 and α-Al_2O_3 increase, as revealed in Fig. 4 (c and e, d and f). It can be inferred that the X-ray penetrating depth in the coating formed without Na_3AlF_6 is larger than that formed with Na_3AlF_6, and Na_3AlF_6 can help to increase the content of the γ-Al_2O_3 and α-Al_2O_3 phase.

3.4 Mechanical properties of the coatings

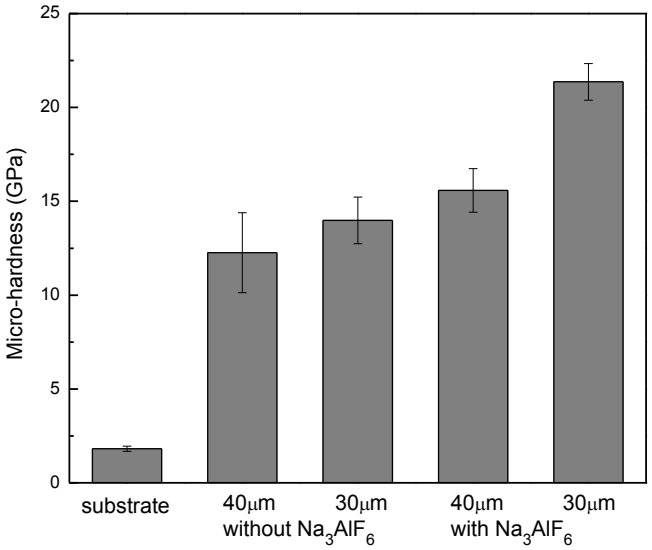

Figure 6. Micro-hardness of substrate and PEO coatings

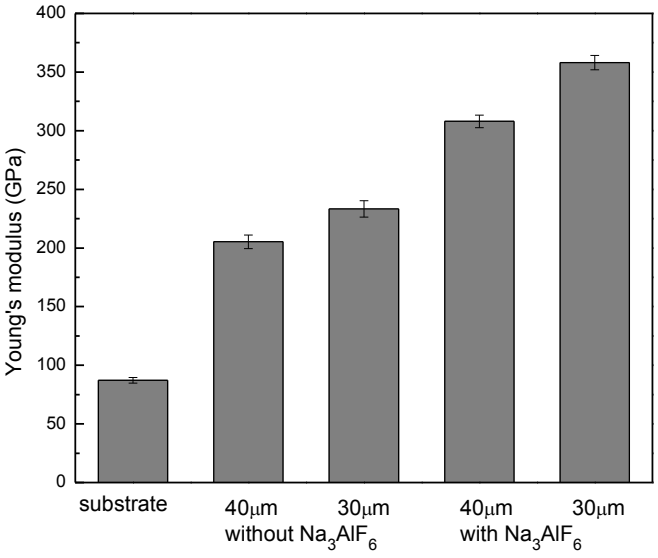

Figure 7. Young's modulus of the 6061 alloy and PEO coatings

Fig. 6 and Fig. 7 compare the micro-hardness and Young's modulus of the 6061 Al alloy and the PEO coatings, It can be seen that the micro-hardness and Young's modulus exhibited by the bare 6061 Al alloy substrate is only 1.816GPa and 87.163GPa, The micro-hardness and Young's modulus of the coatings obtained in electrolyte without Na_3AlF_6 polished to about 40μm and 30μm is 12.259GPa ， 205.248GPa and 13.985GPa， 233.741GPa, respectively[30-32]. In contrast, the PEO coatings obtained in electrolyte with Na_3AlF_6 exhibited much higher micro-hardness and Young's modulus and the value are 15.576GPa， 307.924GPa and 21.363GPa, 358.067GPa, respectively. Such differences in mechanical properties might be due to the different contents of the γ-Al_2O_3 and α-Al_2O_3 phase because

they have different micro-hardness and Young's modulus. Especially for the α-Al_2O_3 phase, it can reach 24.5GPa and 360~400GPa. And thus, the content of the α-Al_2O_3 phase would directly affect the micro-hardness and Young's modulus of the ceramic coatings. From Fig. 5, it can be seen that the content of α-Al_2O_3 and γ-Al_2O_3 of the coatings obtained in electrolyte with Na_3AlF_6 was increased, especially for 30μm, it's the main reason why the highest micro-hardness and Young's modulus presented. As shown in Fig. 3, the PEO coatings obtained in electrolyte with Na_3AlF_6 polished to 30μm is the most compact. The more compact the higher mechanical properties.

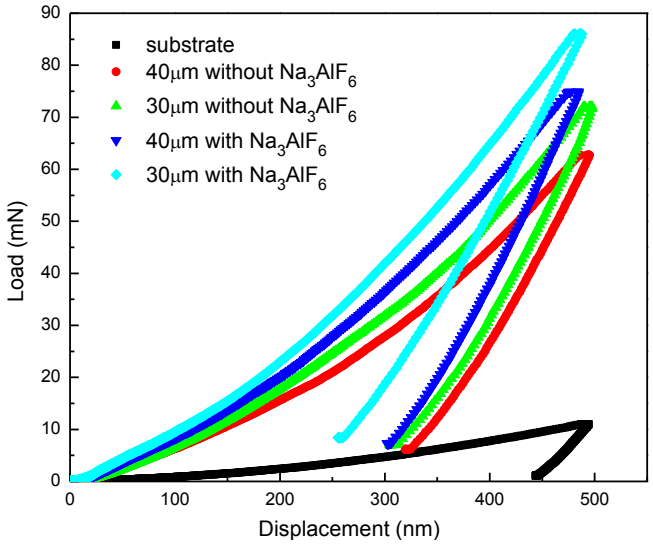

Figure 8. Typical load–displacement curve of the 6061 alloy and PEO coatings

Fig.8 shows a typical load–displacement curve of the 6061 Al alloy and the PEO coatings, It can be seen that the loading and unloading curves are not linear, the results from elastic and plastic deformation. The maximum displacement results from elastic and plastic deformation, with elastic recovery occurring on unloading. The loads applied to reach the same penetration depth of 500 nm were different for the substrate and the PEO coating, 6061 Al alloy required maximum load about 11mN and the elastic recovery was 11.17%, while the PEO coating required maximum load about 62mN and the elastic recovery were over 36.00%. The maximum load of the coatings obtained in electrolyte with Na_3AlF_6 reached 86mN, the elastic recovery reached 48.76%. Micro-hardness and Young's modulus of the coatings were obviously higher than 6061 Al alloy, with the addition of Na_3AlF_6, micro-hardness and Young's modulus were improved obviously.

4. CONCLUSION

The structure and mechanical properties of the PEO coatings formed in electrolyte solution with and without Na_3AlF_6 have been investigated， all the coated specimens have a double-layer structure and a rough porous surface. The Na_3AlF_6 can improve the thickness and compactness;

increase the content of the γ-Al_2O_3 and α-Al_2O_3; improve micro-hardness and Young's modulus. The results showed that when the Na_3AlF_6 in the electrolyte, micro-hardness and Young's modulus of the PEO coatings reached 21.363GPa and 358.067GPa respectively, elastic recovery reached to 48.76%, higher toughness also can be obtained

ACKNOWLEDGEMENT
The authors thank the Supported by Program for New Century Excellent Talents in University (NCET-09-0064), The National Natural Science Foundation of China (No. 51078101) and Space Debris Special (K0202210) for the financial support for this work.

References

1. H.C. Chen, A.J. Pinkerton, L. Li, Z. Liu, A.T. Mistry, *Mater. Des.* 32 (2011) 495-504.
2. M. Elmadagli, T. Perry, A.T. Alpas, *Wear*. 262 (2007) 79-92.
3. K.L. Sahoo, C.S. Sivaramakrishnan, *J.Mater.Process.Technol.* 135 (2003) 253-257.
4. W.R. Osório, N. Cheung, J.E. Spinelli, K.S. Cruz, A. Garcia, *Appl. Surf. Sci.* 254 (2008) 2763–2770.
5. Y.C. Tsai, C.Y. Chou, S.L. Lee, C.K. Lin, J.C. Lin, S.W. Lim, *J. Alloys Compd*. 487 (2009) 157-162.
6. N.P. Wasekar, A. Jyothirmayi, G. Sundararajan, *Int. J. Fatigue.* 33 (2011) 1268-1276.
7. K. Mutombo, M.D. Toit, *Int. J. Fatigue*. 33 (2011) 1539-1547.
8. L.P. Troeger, E.A. Starke Jr, *Mater. Sci. Eng.*, A 277 (2000) 102-113
9. J. Barranco, F. Barreras, A. Lozano, M. Maza, *J. Power Sources*. 196 (2011) 4283-4289.
10. Y. Kyo, A.P. Yadav, A. Nishikata, T. Tsuru, *Corros. Sci*. 53 (2011) 3043-3047.
11. J.A. Picas, A. Forn, R. Rilla, E. Martín, *Surf. Coat. Technol*. 200 (2005) 1178- 1181.
12. X. Li, X. Nie, L. Wang, D.O. Northwood, *Surf. Coat. Technol*. 200 (2005) 1994-2000.
13. A.K. Mukhopadhyay, A.K. Sharma, *Surf. Coat. Technol*. 92 (1997) 212-220.
14. V. Lopez, J.A. Gonzalez, E. Otero, E. Escudero, M. Morcillo, *Surf. Coat. Technol*. 153 (2002) 235-244.
15. F. Snogan, C. Blanc, G. Mankowski, N. Pebere, *Surf. Coat. Technol*. 154 (2002) 94-103.
16. S.H. Awad, H.C. Qian, *Wear*. 260 (2006) 215-222.
17. Z.P. Yao, L. L. Li, Z.H. Jiang, *Appl. Surf. Sci.* 255 (2009) 6724-6728.
18. M.S. Vasilyeva, V.S. Rudnev, A.Y.Ustinov, I.A. Korotenko, E.B. Modin, O.V. Voitenko, *Appl. Surf. Sci.* 257 (2010) 1239-1246.
19. M.R. Bayati, R. Molaei, A.Z. Moshfegh, F. Golestani-Fard. *J. Alloys. Compd*. 509 (2011) 6236-6241.
20. X.H. Wu, W. Qin, Y. Guo, Z.H. Xie, *Appl. Surf. Sci.*254 (2008) 6395-6399.
21. J. He, Q.Z. Cai, H.H. Luo, L. Yu, B.K. Wei, *J. Alloys. Compd*. 471 (2009) 395-399.
22. X.L. Zhang, Z.H. Jiang, Z.P. Yao, Z.D. Wu, *Corros. Sci*. 52 (2010) 3465-3473.
23. M. Laleh, A. Sabour Rouhaghdam, T. Shahrabi, A. Shanghi, *J. Alloys. Compd*. 496 (2010) 548-552.
24. C.H. Hsu, H.P. Teng, F.H. Lu, *Surf. Coat. Technol*. 205 (2011) 3677-3682.
25. G. Sundararajan, L. Rama Krishna, *Surf. Coat. Technol*. 167 (2003) 269-277.
26. G.H. Lv, H. Chen, X.Q. Wang, H Pang, G.L. Zhang, B. Zou, H.J. Lee, S.Z. Yang, *Surf. Coat. Technol*. 205 (2010) S36-S40.
27. H.F. Guo, M.Z. An, *Appl. Surf. Sci*. 246 (2005) 229-238.
28. A.J. Zozulin, D.E. Bartak, *Met. Finish*. 92 (1994) 39-44.

29. A.K. Sharma, R. Uma.R, A. Malek, K.S.N. Acharya, M. Muddu, S. Kumar, *Met. Finish*. 94 (1996) 16-27.
30. Y.L.Wang, Z.H. Jiang, Z. P. Yao, *J. Alloys Compd*. 481 (2009) 725-729.
31. K. Wang, B.H. Koo, C.G. Lee, Y.J. Kim, S.H. Lee, E. Byon, *T. Nonferr. Metal. Soc.* 19 (2009) 866-870.
32. K. Wang, B.H. Koo, C.G. Lee, Y.J. Kim, S.H. Lee, E. Byon, Chinese. J. Aeronaut. 22 (2009) 564-568.